Oscillation Suppression of EO Response in Coherent Driver Modulator for Over 160 Gbaud Operation

Josuke Ozaki, Yoshihiro Ogiso, *Member, IEEE*, Hiroshi Yamazaki, *Member, IEEE*, Yasuaki Hashizume, Mitsuteru Ishikawa, *Member, IEEE*, and Nobuhiro Nunoya, *Member, IEEE*

***Abstract*— We have developed a high-bandwidth coherent driver modulator (HB-CDM) with no oscillation in the electro-optic (EO) response and a 3-dB EO bandwidth exceeding 90-GHz. This can operate at over 160 Gbaud, making it the highest-bandwidth CDM ever reported. To achieve the smooth EO response of the HB-CDM, we adjusted the vertical spatial distance between the driver and the lid inside the package, which determines the cavity resonance frequency. We successfully suppressed EO oscillations by increasing the lid thickness and varying this distance, ensuring that the resonance frequency is above 100-GHz. At this frequency, the normalized EO response is below −20-dB, and the driver's μ-factor is above 1. In addition, we demonstrated up to 168-Gbaud dual-polarization 16-QAM modulations by using the HB-CDM without EO oscillation.**

***Index Terms*— Electrooptic modulation, high-speed optical modulators, indium compounds, digital coherent, quadrature amplitude modulation.**

I. Introduction

COHERENT optical transceivers that can operate at high baud rates are required to increase transmission capacity per wavelength and extend transmission distances in optical transmission systems. Among the key components of optical transceivers, InP modulators [1], thin-film $LiNbO_3$ (TFLN) modulators [2], [3], and SiPh modulators [4] are well-known. InP and TFLN modulators are primarily being researched and developed for high-end applications in metro to long-haul scenarios due to their high bandwidth and low half-wave voltage (V_π). On the other hand, SiPh modulators, although they have inferior bandwidth and driving voltage characteristics compared with the former two, are often used for short-reach low-end applications because of their compact size, affordability, and excellent productivity.

Manuscript received 25 August 2023; revised 22 November 2023; accepted 4 December 2023. Date of publication 8 December 2023; date of current version 15 December 2023. *(Corresponding author: Josuke Ozaki.)*

Josuke Ozaki, Yoshihiro Ogiso, Yasuaki Hashizume, Mitsuteru Ishikawa, and Nobuhiro Nunoya are with the NTT Device Innovation Center, Nippon Telegraph and Telephone Corporation, Atsugi, Kanagawa 243-0198, Japan (e-mail: josuke.ozaki@ntt-devices.com; yoshihiro.ogiso@ntt-devices.com; yasuaki.hashizume@ntt.com; mitsuteru.ishikawa@ntt-devices.com; nobuhiro.nunoya@ntt-devices.com).

Hiroshi Yamazaki is with NTT Device Technology Laboratories, Nippon Telegraph and Telephone Corporation, Atsugi, Kanagawa 243-0198, Japan (e-mail: hrsh.yamazaki@ntt.com).

Color versions of one or more figures in this letter are available at https://doi.org/10.1109/LPT.2023.3339960.

Digital Object Identifier 10.1109/LPT.2023.3339960

The high-bandwidth coherent driver modulator (HB-CDM) [5] is a well-known form factor that utilizes high-speed modulator chips based on InP [6], [7] and TFLN [8]. In the HB-CDM, a driver die and a modulator chip, previously packaged separately, are now assembled next to each other in a single package to enable high-speed operation. Therefore, achieving a smooth RF connection between the modulator and the driver is important. In addition, using a flexible printed circuit (FPC) as the RF interface of the package enables excellent impedance matching and minimized RF losses, and up to 144-Gbaud operation has been reported using the HB-CDM including the InP-based modulator chip [7].

Since the HB-CDM has the driver and modulator in the same package, designing packaging that ensures stable operation of the driver is important to maintain good signal integrity, which is not necessary when packaging the modulator alone. For example, even if the driver die itself does not oscillate, it may become unstable and oscillate due to assembly conditions. The instability and oscillation can lead to undesired oscillations in the electro-optic (EO) characteristics of the HB-CDM, thereby degrading the transmission characteristics.

We report on an HB-CDM that achieves a 3-dB EO bandwidth exceeding 90 GHz, without the EO oscillations. The 3-dB EO bandwidth is sufficient for over 160-Gbaud-class IQ modulation. We have found that it is important to keep the distance between the lid surface and the driver surface in the HB-CDM, which is related to the cavity resonance frequency, short enough to suppress EO oscillations. This letter discusses how this distance should be designed to suppress them. Furthermore, we obtained good back-to-back bit-error-rate (BER) performance in up to 168-Gbaud dual-polarization (DP) 16-QAM modulations with pre-equalization to suppress the excessive peaking of the HB-CDM caused by the driver IC.

II. Fabricated HB-CDM

Fig. 1 shows a photograph of the fabricated HB-CDM with FPC RF interface. The package body size is 12 × 30 × 5.3 mm^3. The HB-CDM includes an InP-based n-i-p-n heterostructure twin-IQ modulator chip with a differential capacitively-loaded travelling-wave electrode (CL-TWE) and a 4-channel linear SiGe BiCMOS driver die with an open-collector configuration. The package and modulator chip used were the same as those previously reported; the characteristics

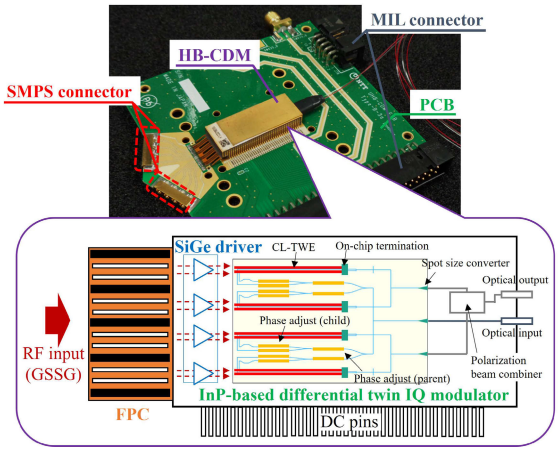

Fig. 1. Photograph and schematic diagram of the fabricated CDM.

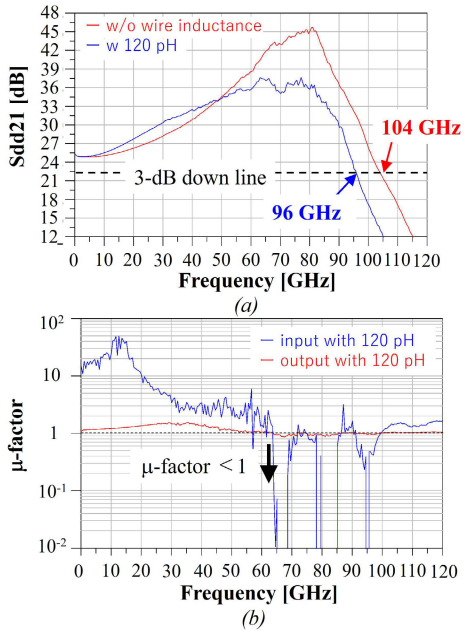

Fig. 2. Driver's measured small-signal electrical characteristics of (a) differential gain (Sdd21) and (b) differential μ-factor.

of the package and modulator chip are an electrical (EE) 3-dB bandwidth of 80 GHz and a roll-off frequency of over 100 GHz, and a 3-dB bandwidth of over 72 GHz with V_π of 2 V, respectively [7].

Fig. 2 shows the measured differential gain Sdd21 (Fig. 2(a)) and the differential μ-factor [9] (Fig. 2(b)) of the driver. The S-parameters are re-normalized to an input and output port impedance of differential 100 Ω and 60 Ω, respectively. These measurements simulate the impedance of the package connected to the driver (input port) and modulator (output port), respectively. In Fig. 2(a), the red line shows the driver characteristics alone, while the blue line shows the schematic simulation results when 120 pH is added to the input and output of the measured S-parameter, accounting for the wire connection between the driver and the package or the modulator. The driver alone exhibits a 3-dB EE bandwidth of 104 GHz, which reduces to 96 GHz with the inclusion of 120-pH wire inductance. In our assembly conditions, the wire inductance was controlled to be less than 120 pH, and the driver is designed to have sufficient RF characteristics

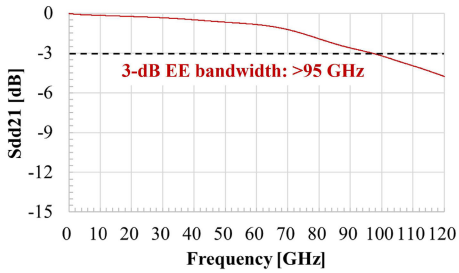

Fig. 3. Differential insertion loss (Sdd21) of evaluation board.

even with 120 pH. Even with the inductance of 120 pH, the magnitude of the peaking at 80 GHz exceeds 10 dB, which is more than the sum of the RF losses (approximately −7 dB at 80 GHz) of our modulator chip (about −4 dB at 80 GHz) and the package (about −3 dB at 80 GHz) [7], which can achieve an HB-CDM with bandwidth above 80 GHz supporting 160 Gbaud operations. While sufficient bandwidth can be achieved, the EO response of the HB-CDM will have excessive peaking due to driver peaking. To achieve better transmission characteristics, it is desirable to suppress the driver's peaking amplitude to be comparable to the overall losses. To achieve a higher bandwidth HB-CDM with this driver, it is effective to reduce the inductance by increasing the number of wires or using flip-chip connections. The μ-factor of both the input (blue) and output sides (red) with 120 pH is shown in Fig. 2(b). The μ-factor of both the input and output remains around or below 1 in the 60–100 GHz range, indicating that the driver is conditionally stable in this frequency range and that there is a risk of the driver oscillating, depending on the assembly conditions in the HB-CDM. In addition, the output amplitude with a differential load of 60 Ω was 2.5 V_{ppd} and the total power consumption of the 4 channels was approximately 3 W.

As shown in Fig. 1, the HB-CDM is soldered to a printed circuit board (PCB) that has a 100-GHz compatible sub-miniature push-on (SMPS) connector as the RF interface and a United States Military Standard (MIL)-based connector, conforming to the MIL-C-83503 standard, as the DC power interface. A small 4-channel SMPS connector with a channel pitch of 3 mm was used. If a 1 mm end-launch connector were used, the channel pitch would be almost three times that of this 4-channel integrated connector. The use of this small RF connector is very useful in terms of shortening the length of the RF transmission line and reducing RF losses on the PCB. Fig. 3 shows the differential insertion loss, which includes the losses of the RF transmission line on the PCB after 2.5 mm from the edge of the FPC pad for connection to the PCB and the RF connectors. The 3-dB EE bandwidth of the evaluation board is over 95 GHz, and the roll-off frequency exceeds 110 GHz. This demonstrates very low RF loss and the capability for over 160 Gbaud operation.

III. Experimental Result

A. Small-Signal EO Response and Oscillation

Fig. 4(a) shows the small-signal EO responses of the fabricated HB-CDM without the evaluation board RF losses shown in Fig. 3. The EO response is measured by lightwave components analyzers, and the data is normalized at 1 GHz.

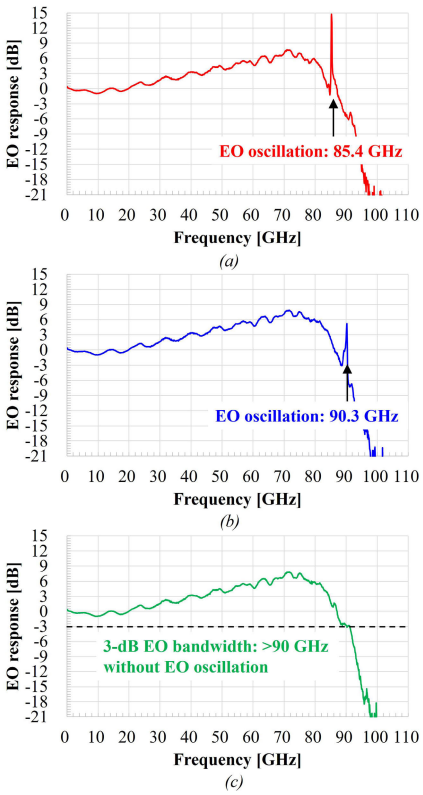

Fig. 4. HB-CDM's small-signal EO response with distances between the driver and lid of (a) 1.75 mm, (b) 1.6 mm and (c) 1.35 mm.

A large oscillation is observed around 85 GHz. Oscillations in the small-signal response also occur when driven by large signals, such as in IQ modulation, leading to degradation in transmission characteristics, such as bit error rates. The cause of the EO oscillation around 85 GHz is that the cavity resonance frequency, due to the spatial vertical distance between the driver and the lid, matched with the frequency range with the driver's μ-factor below 1, where the driver is conditionally stable. Therefore, we considered that the oscillation could be suppressed by shifting the cavity resonance frequency to a higher frequency than the required frequency bandwidth, where the driver's both the input and output μ-factor is larger than 1, such as between 100 and 120 GHz as shown in Fig. 2(b). In general, cavity resonance occurs when an integer multiple of $\lambda/2$ standing waves is generated in the cavity, where λ represents the wavelength of the electromagnetic wave at the resonant frequency. This means that EO oscillations can occur at a frequency equal to twice the cavity distance in either direction within the HB-CDM. Considering the electromagnetic field of the driver, we focused on the distance from the driver surface to the lid surface as the cavity resonance point.

Fig. 5(a) shows a vertical cross-sectional view of the fabricated HB-CDM, whose EO responses were shown in Fig. 4(a). The distance between the driver and the lid of the HB-CDM was approximately 1.75 mm. The observed oscillation frequency in Fig. 4(a) is 85.4 GHz, which corresponds to $\lambda = 3.51$ mm in air. This indicates that cavity resonance will occur if there is a space where a standing wave of $\lambda/2 = 1.755$ mm is generated. This value is almost equal to the vertical distance between the driver and the lid.

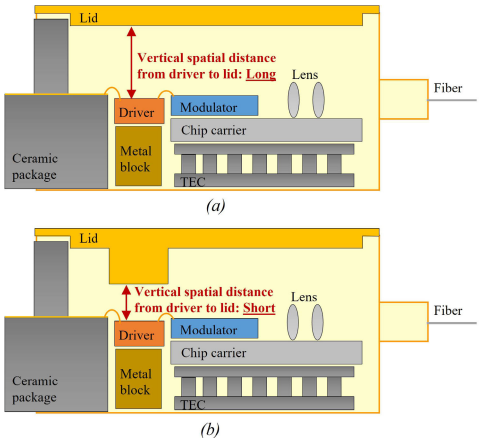

Fig. 5. Vertical sectional diagram of HB-CDM showing spatial distance between the driver and lid with (a) conventional thin lid and (b) thick lid.

To investigate the effect of the distance between the driver and the lid on the oscillation in the EO response of the HB-CDM, we varied the distance by using lids of different thicknesses with the same HB-CDM. Figs. 5(a) and (b) show diagrams of a conventional thin lid and thick lid used to suppress the oscillation, respectively. To vary only the spatial vertical distance between the driver and lid, the lid was thickened only above the driver, as shown in Fig. 5(b). In other aspects of the assembly, numerous short ground wires were bonded to minimize the driver instability. Figs. 4(a), (b), and (c) shows the results of the EO responses measured using three different lid thicknesses and varying the distance between the driver and the lid. In Figs. 4(a), (b), and (c), the distances are 1.75, 1.6 and 1.35 mm, and the vertical cavity resonant frequencies are expected to be 85.6, 93.7 and 111.0 GHz, respectively. As the distance between the driver and lid decreases, the calculated resonance frequency shifts toward the high-frequency side, and the same trend is observed in the measured EO response. The oscillation frequency confirmed by the EO response at a distance of 1.6 mm is 90.3 GHz, as shown in Fig. 4(b), which is comparable to the calculated resonance frequency. Fig. 4(c) shows that the EO oscillations can be suppressed by setting the spatial distance appropriately so that the cavity resonance frequency is higher than the frequency at which the EO response is at least below -20 dB, and the μ-factor is larger than 1; in this HB-CDM, this means that the distance should be such that the cavity resonant frequency exceeds 100 GHz. A distance of 1.35 mm (corresponding to a frequency of 111 GHz) has a margin of about 10% from the minimum required distance of 1.5 mm (corresponding to a frequency of 100 GHz), indicating that the EO oscillation can be suppressed even when assembly variations occur. Furthermore, in Fig. 4(c), where the oscillation is suppressed, no degradation of the EO characteristics exists due to the closer distance, and the 3-dB EO bandwidth exceeds 90 GHz, which, to our knowledge, is the highest 3-dB EO bandwidth reported for any HB-CDM to date. In addition, this configuration, which changes the distance only at the top of the driver without interference from other components, is useful for reducing the distance to achieve a higher bandwidth CDM. Thus, HB-CDMs with internally integrated driver ICs have a risk of EO oscillation if the driver has frequencies where the μ-factor <1, and the

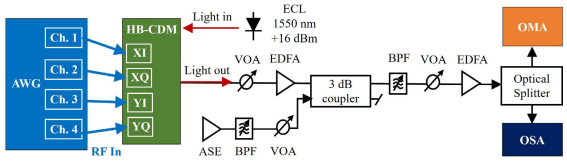

Fig. 6. Experimental setup for back-to-back IQ modulations.

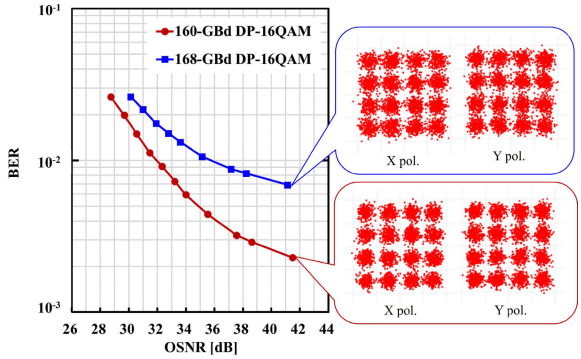

Fig. 7. BER characteristics and constellation diagram of 160 Gbaud DP-16QAM and 168 Gbaud DP-16QAM modulations.

oscillation can be suppressed by the assembly conditions. In detail, by controlling the cavity resonant frequencies away from the frequencies where the μ-factor <1, we can achieve smooth EO characteristics (without EO oscillation) and high baud-rate operation. Moreover, if the driver is stable (μ-factor >1) near the cavity resonance frequencies, the EO oscillation is not observed even in the same package with a distance of 1.75 mm [7].

B. IQ Modulation

Fig. 6 shows the experimental setup for back-to-back IQ modulations. The HB-CDM without EO oscillation was used. The insertion loss per polarization and the static extinction ratio of the HB-CDM were less than 8 dB and over 28 dB for both child and parent Mach-Zehnder interferometers, respectively. A light source with a linewidth of <100 kHz was used at a wavelength of 1550 nm and a power of $+16$ dBm. A 256 GS/s arbitrary waveform generator (AWG) with a DAC having a 3-dB analog bandwidth of more than 80 GHz was used as the RF signal source, and an optical modulation analyzer (OMA) with a 3-dB analog bandwidth of >100 GHz was used at the receiver end. The AWG and the SMPS connectors on the PCB were connected by an RF cable with a total length of about 25 cm. An erbium-doped fiber amplifier (EDFA) and a variable optical attenuator (VOA) were used to maintain the optical signal power at a constant value. An amplified spontaneous emission (ASE) noise source and a 5.5-nm bandpass filter (BPF) were used to control the received optical signal-to-noise ratio (OSNR). The optical output spectrum through a 3-nm BPF was measured with an optical spectrum analyzer (OSA) for the OSNR measurements.

Fig. 7 shows the back-to-back pre-FEC (forward error correction) BER performance and the constellations of 160-Gbaud DP-16QAM (red) and 168-Gbaud DP-16QAM (blue) modulations. The OSNR was measured in a 0.1-nm reference noise bandwidth. The RF signals from the AWG were pulse-shaped using a root-raised-cosine (RRC) filter with a roll-off factor of 0.1. The modulator bias was set to obtain a V_π of 2.0 V. The optical output power was approximately -8.5 dBm, and the modulation loss was about 14 dB, excluding the 3-dB quadrature loss, which means that the modulation depth would be about 30%. On the transmitter side, linear digital pre-equalization was performed to compensate for both the RF cable losses and the excessive peaking in the EO response caused by the driver. On the receiver side, an ordinary adaptive equalizer controlled by the decision-directed least-mean-square algorithm was used. We observed clear constellations of both 160-Gbaud DP-16QAM and 168-Gbaud DP-16QAM modulations. The measured BERs at the best OSNR of 41.5 dB for the 160-Gbaud DP-16QAM and 41.1 dB for the 168-Gbaud DP-16QAM were 2.3×10^{-3} and 6.9×10^{-3}, respectively. These results confirm that the HB-CDM has sufficient EO characteristics for operation in the 160 Gbaud class and above.

IV. Conclusion

This study investigated causes of EO oscillations in an HB-CDM and the means to suppress the oscillation. Assuming that the cavity oscillation is influenced by the vertical spatial distance between the driver and lid inside the package, the EO oscillation could be successfully suppressed by thickening the lid above the driver and setting the cavity resonance frequency to be sufficiently outside the required bandwidth. As a result, the HB-CDM achieved a 3-dB EO bandwidth of more than 90 GHz and exhibited smooth EO characteristics without any oscillations. We also successfully demonstrated modulations up to 168-Gbaud DP 16-QAM, which is the fastest operating baud rate reported to date using an HB-CDM.

References

[1] Y. Ogiso, J. Ozaki, Y. Hashizume, and M. Ishikawa, "High-bandwidth InP MZ/IQ modulator PIC ready for practical use," in *Proc. Eur. Conf. Opt. Commun. (ECOC)*, Basel, Switzerland, Sep. 2022, pp. 1–3.

[2] M. Xu and X. Cai, "Advances in ultra-wideband $LiNbO_3$ thin-film modulators," in *Proc. Opt. Fiber Commun. Conf. Exhib. (OFC)*, San Diego, CA, USA, Mar. 2023, pp. 1–3, doi: 10.1364/OFC.2023.Tu3C.1.

[3] M. Zhang, C. Wang, P. Kharel, D. Zhu, and M. Lončar, "Integrated lithium niobate electro-optic modulators: When performance meets scalability," *Optica*, vol. 8, no. 5, p. 652, May 2021, doi: 10.1364/optica.415762.

[4] Y. Shi et al., "Silicon photonics for high-capacity data communications," *Photon. Res.*, vol. 10, no. 9, p. A106, Sep. 2022, doi: 10.1364/prj.456772.

[5] (Jul. 2021). *Implementation Agreement for the High Bandwidth Coherent Driver Modulator (HB-CDM)*. IA # OIF-HB-CDM-02.0. [Online]. Available: https://www.oiforum.com/wp-content/uploads/OIF-HB-CDM-02.0.pdf

[6] J. Ozaki et al., "500-Gb/s/λ operation of ultra-low power and low-temperature-dependence InP-based high-bandwidth coherent driver modulator," *J. Lightw. Technol.*, vol. 38, no. 18, pp. 5086–5091, Sep. 15, 2020, doi: 10.1109/JLT.2020.2998466.

[7] J. Ozaki et al., "Over-85-GHz-bandwidth InP-based coherent driver modulator capable of 1-Tb/s/λ-class operation," *J. Lightw. Technol.*, vol. 41, no. 11, pp. 3290–3296, Jun. 15, 2023, doi: 10.1109/JLT.2023.3236962.

[8] S. Makino, S. Takeuchi, S. Maruyama, M. Doi, Y. Ohmori, and Y. Kubota, "Demonstration of thin-film lithium niobate high-bandwidth coherent driver modulator," in *Proc. Opt. Fiber Commun. Conf. Exhib. (OFC)*, San Diego, CA, USA, Mar. 2022, pp. 1–3.

[9] M. L. Edwards and J. H. Sinsky, "A new criterion for linear 2-port stability using a single geometrically derived parameter," *IEEE Trans. Microw. Theory Techn.*, vol. 40, no. 12, pp. 2303–2311, Dec. 1992, doi: 10.1109/22.179894.